Structure of ^{22}Mg and its implications for explosive nucleosynthesis

A. A. Chen,* R. Lewis, K. B. Swartz,† D. W. Visser, and P. D. Parker
Wright Nuclear Structure Laboratory, Yale University, New Haven, Connecticut 06520-8124
(Received 22 January 2001; published 22 May 2001)

The locations of ^{18}Ne+α resonances have been measured as excited states in ^{22}Mg using the ^{12}C(^{16}O,^{6}He)^{22}Mg reaction. Eighteen new levels were discovered in the range $0 \leqslant E_{\mathrm{c.m.}} \leqslant 3$ MeV above the ^{18}Ne+α threshold. The ^{18}Ne$(\alpha,p)^{21}$Na reaction rate in the temperature range $0.2 \leqslant T \leqslant 1.0$ GK has been calculated using the results from the present measurements, and the implications for nuclear burning in explosive stellar scenarios are discussed. This study also yielded energy-level information on low-lying ^{21}Na + p resonances of importance to the ^{21}Na$(p,\gamma)^{22}$Mg reaction, one of the key links in the NeNa cycles in novae.

DOI: 10.1103/PhysRevC.63.065807 PACS number(s): 26.30.+k, 24.30.Gd, 25.70.Hi, 27.30.+t

I. INTRODUCTION

In current models of x-ray bursters and nova explosions, the energy generation and nucleosynthesis at temperatures of $T \leqslant 0.4$ GK are determined by the Hot-CNO cycle [1]. As the temperature and density on the surface of the accreting star increase, however, α-particle and proton capture reactions on the Hot-CNO nuclei become faster than the corresponding β^+ decays. In x-ray bursters, the star may then break out of the Hot-CNO to the *rp* process, providing a way to enhance the rate of energy generation and to trigger the subsequent explosion. Based on present nuclear physics information, the initial breakout path is thought to proceed primarily through the ^{15}O$(\alpha,\gamma)^{19}$Ne reaction, but at $T \geqslant 0.8$ GK, another bridge to the *rp* process becomes available to the star through the ^{18}Ne$(\alpha,p)^{21}$Na reaction [2], bypassing the ^{15}O(α,γ) path via the sequence ^{14}O$(\alpha,p)^{17}$F$(p,\gamma)^{18}$Ne$(\alpha,p)^{21}$Na. The contribution of these reactions to the total flux through this mass region depends on their cross sections under extreme stellar conditions. Presently, the ^{18}Ne$(\alpha,p)^{21}$Na reaction rate is not well established experimentally at the relevant temperatures, and hence its contribution to the breakout flow is poorly known.

At the energies found in these explosive environments, most of the reactions of interest proceed through individual resonances above the particle threshold in the compound system. The rates of these reactions as a function of temperature under stellar conditions depend then on the properties of such resonances. The ^{18}Ne$(\alpha,p)^{21}$Na reaction, in particular, is currently a subject of investigation at radioactive beam facilities such as Louvain-la-Neuve and Argonne National Laboratory. Initial direct studies of this reaction have recently been carried out at Louvain-la-Neuve with a radioactive ^{18}Ne beam [3], where resonance locations and strengths in ^{22}Mg were determined for $E_x(^{22}\mathrm{Mg}) > 10.5$ MeV, corresponding to $T \geqslant 1.5$ GK. In the energy region corresponding to lower stellar temperatures, however, only two states in ^{22}Mg above the α-particle threshold at $E_x = 8.14$ MeV and below 10.5 MeV, have been reported in other studies, and their spectroscopic properties are unknown [4] (Fig. 1). A statistical-model calculation has been performed giving a rate in reasonable agreement with that derived from the Louvain results [5] at high temperatures. However, the sparse structure information and the low density of relevant states in the energy region $8.14 \leqslant E_x \leqslant 10.5$ MeV, prevent an accurate calculation of the reaction rate for $T < 1.5$ GK. Moreover, based on the structure of the isospin mirror ^{22}Ne, there are about 22 missing states in this region. Radioactive beam experiments aiming to measure the cross section directly can benefit greatly from a foreknowledge of the location of key resonances.

While breakout from the Hot-CNO cycle supplies the energy trigger for x-ray bursts, our present understanding of explosive nucleosynthesis in novae indicates that the temperature on the surface of the accreting white dwarf is too low for breakout to occur. For ONeMg novae, the sources of energy for the thermonuclear runaway are instead the NeNa and MgAl cycles [1]. In the NeNa cycles, the reaction ^{21}Na$(p,\gamma)^{22}$Mg is especially important because it bypasses the ^{21}Na β decay, resulting in greater energy generation during the explosion. Furthermore, the reaction plays a key role in determining the final abundance of ^{22}Na produced in the nova nucleosynthesis. Since the decay of ^{22}Na is followed by the emission of a 1.27 MeV γ ray, the abundance of ^{22}Na in the material ejected by the explosion could be inferred from measurements of the γ-ray flux, and thereby used as a constraint for nova models [6], provided the nucleosynthetic cross sections for the production and destruction of ^{22}Na are understood. Additionally, in carbonaceous meteoritic grains, the beta-decay daughter of ^{22}Na, ^{22}Ne, has been found to be enriched relative to ^{20}Ne by more than a factor of 100 compared to the solar abundance; the total yield of ^{22}Na is needed in attempts to establish the formation site of such grains [7]. As with the ^{18}Ne$(\alpha,p)^{21}$Na reaction, at relevant temperatures, the ^{21}Na$(p,\gamma)^{22}$Mg rate is expected to be dominated by individual resonances in ^{22}Mg, as shown in the energy-level diagram in Fig. 2, and the present rate is based on estimates of their spectroscopic properties [8–10]. However, a recent measurement of the ^{24}Mg$(p,t)^{22}$Mg reac-

*Present address: TRIUMF, 4004 Wesbrook Mall, Vancouver, British Columbia, Canada V6T 2A3.
†Present address: BD Immunocytometry Systems 2350, Qume Drive, San Jose, CA 95131.

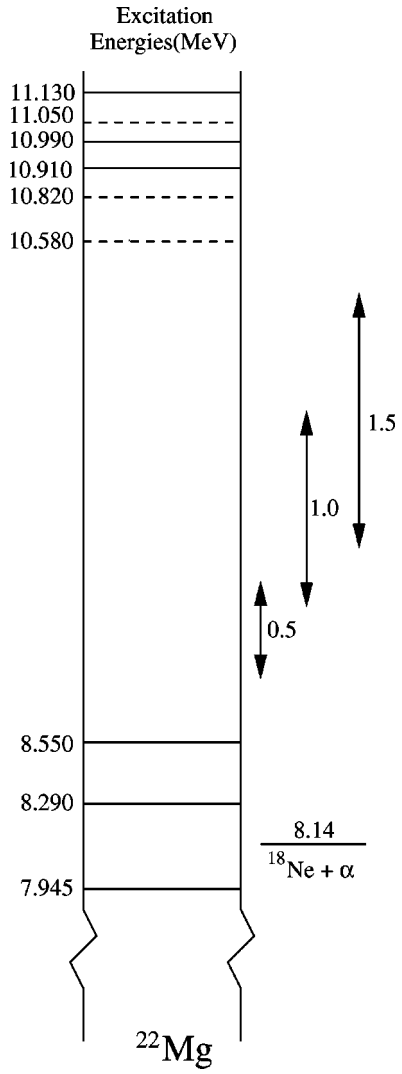

FIG. 1. Previously known energy levels of relevance to the ^{18}Ne$(\alpha,p)^{21}$Na reaction. The first two levels above the threshold were observed in Ref. [14]. The levels at excitation energies above 10.5 MeV were seen in the direct measurement of the ^{18}Ne$(\alpha,p)^{21}$Na reaction rate by Bradfield-Smith and collaborators [3]. The levels shown as dashed lines were assigned tentatively. The Gamow windows for temperatures of 0.5, 1.0, and 1.5 GK are displayed as double arrows.

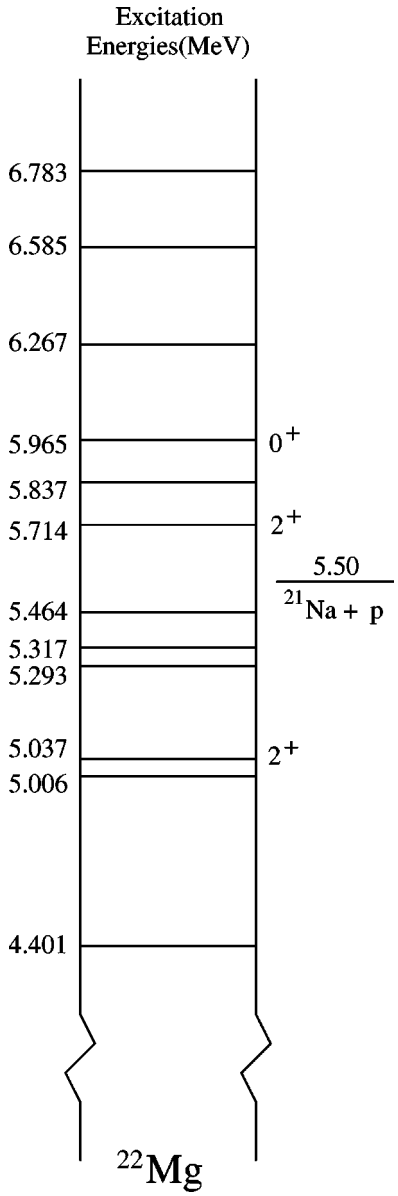

FIG. 2. Previously known energy levels of relevance to the ^{21}Na$(p,\gamma)^{22}$Mg reaction. The energies are taken from the $A=22$ energy-level compilation in Ref. [4]. The first three levels above the ^{21}Na$+p$ threshold have been expected to be the main contributors to the reaction rate at nova temperatures ($T \lesssim 0.4$ GK).

tion [11] has resulted in apparent contradictions with some of the accepted energy levels [4], and the existence of missing states cannot be discounted. Until the reaction cross section is measured directly (e.g., ISAC-TRIUMF), an independent check of these discrepancies would be useful.

With this in mind, we have used the ^{12}C(^{16}O, ^{6}He)^{22}Mg reaction to measure the location of resonances in ^{22}Mg of importance to the ^{18}Ne$(\alpha,p)^{21}$Na and ^{21}Na$(p,\gamma)^{22}$Mg reactions, and report on our results in the following sections.

II. EXPERIMENTAL SETUP

The structure of ^{22}Mg had thus far been studied primarily through the (p,t), $(^{3}\mathrm{He},n)$, and $(^{3}\mathrm{He},n\gamma)$ two-nucleon transfer reactions. These reactions proceed mainly through the direct reaction mechanism and tend to selectively populate states of natural parity in ^{22}Mg. Although much progress has been made in determining the structure of ^{22}Mg through these experiments, including the recent remeasurement of the ^{24}Mg$(p,t)^{22}$Mg reaction [11], the spectroscopic information needed for astrophysics studies is still incomplete, as emphasized already. Hence, additional studies with reactions proceeding through different mechanisms, and therefore having a different selectivity, could shed further light on the location of key resonances in ^{22}Mg of relevance to explosive nucleosynthesis.

One such reaction is the ^{12}C(^{16}O, ^{6}He)^{22}Mg. Unlike the two-nucleon transfer reactions, it is expected to proceed primarily through the compound-nucleus reaction mechanism.

The ^{12}C(^{16}O, ^{6}He)^{22}Mg reaction should populate natural-parity states preferentially. This follows because both the ^{12}C and the ^{16}O nuclei have $J^{\pi}=0^{+}$ ground states and therefore the ^{28}Si compound nucleus will be formed in natural-parity states primarily. Since the ejectile ^{6}He also has $J^{\pi}=0^{+}$, natural-parity states in ^{22}Mg are favored in this compound nucleus breakup channel. For the ^{21}Na$+p$ channel, this feature is a problem, since there may be astrophysically important unnatural-parity states that may be populated only weakly at best. (This question is currently being addressed in a study of the ^{25}Mg(^{3}He, ^{6}He)^{22}Mg reaction [12].) For the ^{18}Ne(α,p) reaction, however, only natural-parity $T=1$ states will contribute to the reaction rate anyway, so this selectivity is a help instead of a hindrance.

The Yale ESTU tandem accelerator and the split-pole spectrometer with its focal plane detector system, are ideal for studying heavy-ion reactions such as the ^{12}C(^{16}O, ^{6}He)^{22}Mg. Our group has had experience in these studies through measurements of several other reactions, including the ^{12}C(^{12}C, ^{6}He)^{18}Ne reaction [13] whose dynamics are very similar to that of the ^{12}C(^{16}O, ^{6}He)^{22}Mg reaction. The experiment was performed using a 90-MeV ^{16}O beam produced by the Yale ESTU tandem accelerator. The beam energy of 90 MeV ($E_{\mathrm{c.m.}}=38.6$ MeV) was chosen after taking into account the reaction Q value of -21.93 MeV, the Coulomb barrier of about 20 MeV, and our aim to populate states in ^{22}Mg up to excitation energies of 11 MeV. This last criterion would enable us to check independently the results from the Louvain-la-Neuve measurement of the ^{18}Ne$(\alpha,p)^{21}$Na reaction mentioned earlier.

Natural carbon targets (98.9% ^{12}C and 1.1% ^{13}C) of thickness 20 μg/cm^2 were bombarded with the ^{16}O beam, with typical intensities of 200 particle nA. This target thickness was a compromise between a reasonable differential energy loss in the target and an adequate event rate at the focal plane. The difference in energy loss in the target between the 90-MeV ^{16}O beam (77 keV/ 20 μg cm^{-2}) and the 35-MeV ^{6}He ions (5 keV/ 20 μg cm^{-2}) is about 70 keV/ 20 μg cm^{-2}. This corresponds to a difference of 60 keV between a ^{6}He particle produced at the front of the target and one produced at the back, which is equivalent to a spread of about 30 keV in excitation energy in ^{22}Mg. Fresh target spots were moved into position roughly every 8 h, as they were observed to get visibly thicker due to carbon buildup.

The reaction products were measured at angles of 3°, 5°, 7.5°, and 10° in the laboratory frame. The ^{12}C$+^{16}$O reaction products were momentum analyzed in an Enge split-pole magnetic spectrometer. The solid angle used in the present ^{12}C(^{16}O, ^{6}He)^{22}Mg experiment was selected to give the best balance between energy resolution and count rate. Typically the horizontal slits were set to $\theta=\pm 30$ mrad and the vertical slits to $\phi=\pm 40$ mrad, resulting in an acceptance of $\Delta\Omega=4.8$ msr.

After the momentum analysis in the magnetic spectrometer, the reaction products were measured in the focal plane detector which is a hybrid unit, including two position-sensitive wire assemblies (separated by 10 cm) which determine the momentum and angle of each ion as it enters the chamber. The active length of each wire is surrounded by a series of split u-shaped pickup pads, with 2.5 mm segmentation. The pads nearest to the avalanche location collect the induced charge into a pulse. Each pad is in turn connected to a delay line consisting of 26 tapped-lumped delay-line chips. The position of the particles as they cross each wire assembly is then determined by measuring the relative delay between the pulses arriving at each end of the delay line.

The segmented ionization chamber of the focal plane detector was used to measure the energy deposited by the particles in the gas volume (isobutane at $p=150$ torr) for purposes of particle identification. In the present study, the energy loss in the gas ΔE, was measured with a cathode plate spanning the entire length and depth of the detector. For our measurement, the ^{6}He nuclei of interest are energetic enough to pass through the active volume of the detector and subsequently stop in a 6.35-mm thick plastic scintillator (BC-404) with gain-matched photomultiplier tubes at each end, providing a measurement of the residual energy.

III. DATA ANALYSIS

Since the ^{12}C(^{16}O, ^{6}He)^{22}Mg reaction involves interactions between two α-cluster nuclei in the entrance channel, the cross section for the (^{16}O, α) reaction channel is especially large. The key to isolating the ^{6}He groups of interest from the α particles, about 10^6 times more intense than the ^{6}He group, is the use of the momentum parameter given by the detector front wire signal in conjunction with the E-ΔE discrimination provided by the gas counter and the plastic scintillator.

In addition to the (front-wire vs rear-wire) software gate, software gates were also set on the ^{6}He group in the (cathode vs scintillator), (scintillator vs front-wire), (cathode vs front-wire) histograms. The ^{6}He momentum (or energy) spectrum was obtained by projecting the ^{6}He events that pass through all four gates onto the momentum (position) axis. The position resolution of the projected ^{6}He events was improved by using ray tracing to correct for the $(dp/d\theta)$ broadening.

The ^{6}He position spectra for spectrometer angles of 3°, 5°, 7.5°, and 10° are shown in Figs. 3 and 4. The energy resolution was about 85 keV in E_x(^{22}Mg) and was limited by the focal plane detector. The peaks correspond to excited states in the recoil nucleus ^{22}Mg and are labeled with the E_x. Potential contributions due to ^{13}C were measured using a ^{13}C target and were found to be negligible; no other contaminants were observed. Our criteria for identifying peaks in ^{22}Mg were that a state of a given excitation energy should be observed in at least two angles, and contain a minimum of 40 counts after background subtraction.

At present, the structure of ^{22}Mg is not sufficiently well known to allow for an internal energy calibration of the spectra over the entire energy range ($E_x=1-11$ MeV). An energy calibration for the ^{22}Mg levels was therefore performed for the 5° data by assuming the literature values given for the first and second excited states at $E_x=1.2463$ MeV ± 0.6 keV and 3.3082 MeV± 0.8 keV [4]. Since these two states were strongly populated in the ^{12}C(^{16}O,^{6}He)^{22}Mg re-

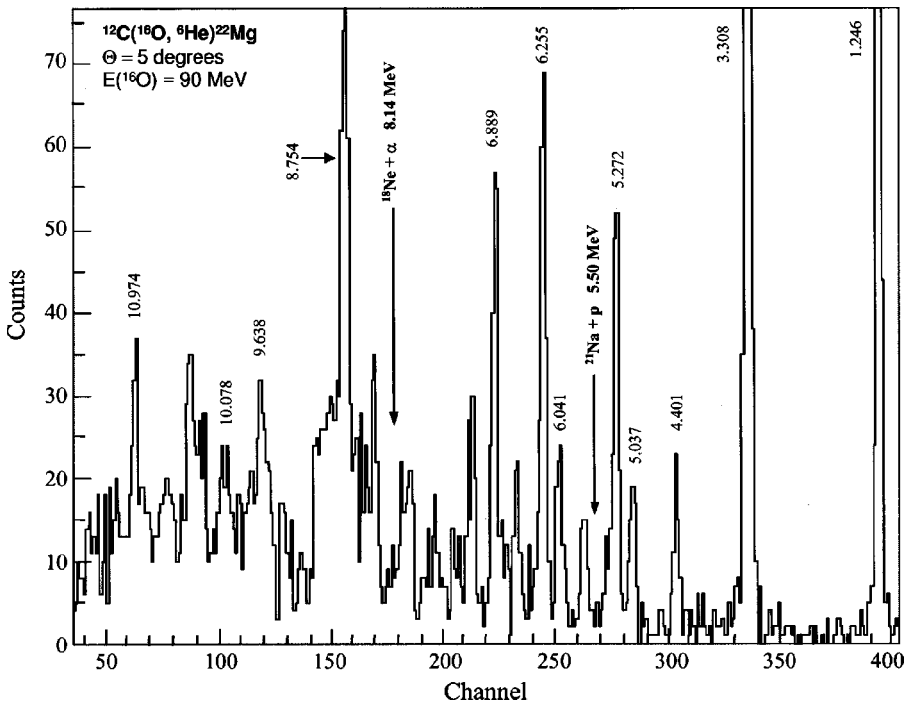

FIG. 3. Energy spectrum from the ^{12}C(^{16}O, ^{6}He)^{22}Mg reaction at 5°. The states with asterisks were used in the energy calibration (see text for details).

action, three different beam energies (76, 84, 90 MeV) were chosen in order to place these two strong peaks at different locations, covering the entire focal plane. (At 76 MeV, the ^{6}He group corresponding to the 3.308 MeV state has the same rigidity as ^{6}He's corresponding to $E_x \approx 10.85$ MeV at a beam energy of 90 MeV.) In this way the calibration of the focal plane was tied directly to the well-established calibration of the facility's 90° beam-analyzing magnet.

In addition to these calibration points, several other known levels from the 90 MeV, $\theta = 5°$ spectrum with excitation energies between 4–6 MeV were included in the calibration. With this calibration, the most accurate energy centroids were determined to within 10–20 keV. The final uncertainty included contributions from the uncertainty in the beam energy centroid ($\leqslant 0.05\%$ of E_{beam}), the experimental errors in the energies listed in the literature, and the uncertainty in the channel centroid from the peak-fitting procedure. The energies obtained from the calibration of the 5° data were then used to internally calibrate the spectra from the other three angles.

IV. RESULTS

A. Resonances in ^{22}Mg: $E_x \geqslant 8.14$ MeV

As seen in the spectra in Figs. 3 and 4, the ^{12}C(^{16}O, ^{6}He)^{22}Mg reaction populates a large number of states in the region above the α-particle threshold ($E_x \geqslant 8.14$ MeV) in ^{22}Mg. We observe a total of 23 levels above 8.14 MeV, as listed in Table I and displayed in Fig. 5. Of these 23, 18 are previously unobserved states. Table I also presents a comparison between these results and previous energies from studies of the ^{20}Ne(^{3}He, n)^{22}Mg transfer reaction [14], and the direct study of the ^{18}Ne(α, p)^{21}Na reaction performed recently at Louvain-la-Neuve [3]. The states observed in the present study at $E_x = 10.570(25)$, 10.844(38), 10.980(31), and 11.135(40) MeV, are in good agreement with the Louvain-la-Neuve ^{18}Ne(α, p)^{21}Na measurements of $E_x = 10.580(50)$, 10.820(60), 10.990(50), and 11.130(50) MeV.

B. Resonances in ^{22}Mg: $E_x \leqslant 8.14$ MeV

Table II displays states in ^{22}Mg found in the energy region below $E_x = 8.14$ MeV. Our results are compared with levels observed in the TRIUMF-CNS measurement of the ^{24}Mg(p, t)^{22}Mg reaction [11], the ^{20}Ne(^{3}He, $n\gamma$)^{22}Mg study by Rolfs *et al.* [15], and the presently accepted energies from the literature [4]. The last reference incorporates results from all previous studies of ^{22}Mg before the present work and the TRIUMF-CNS (p, t) measurement. We have confirmed the existence of a state at 6.04 MeV (also observed by the TRIUMF-CNS Collaboration); our excitation energy of 6.041(11) MeV agrees well with their value of 6.046(3) MeV. Their measurement also revealed another level at 5.962 MeV, which we have not observed. The latest $A = 22$ energy-level compilation [4] lists only one state in the 5.9–6.0 MeV region (at 5.965 MeV); this energy was deduced by averaging the energies of states seen in a number of studies involving two-nucleon transfer reactions [14–17]. Based on the accuracy of those measurements and the observed angular distributions alone, one cannot determine unambiguously whether or not these previous measurements lend support to the existence of one or two states near 6.0 MeV.

New levels were found in the present study at $E_x = 7.402$, 7.674, and 8.062 MeV; the present study did not observe previously reported states at $E_x = 5.006$ MeV, 5.317 MeV, and 5.837 MeV. For states between $E_x = 6$ and 8 MeV, the present results are in reasonable agreement with the previously adopted values as listed in Table II. With regards to analog states in ^{22}Ne, the original assignments for levels

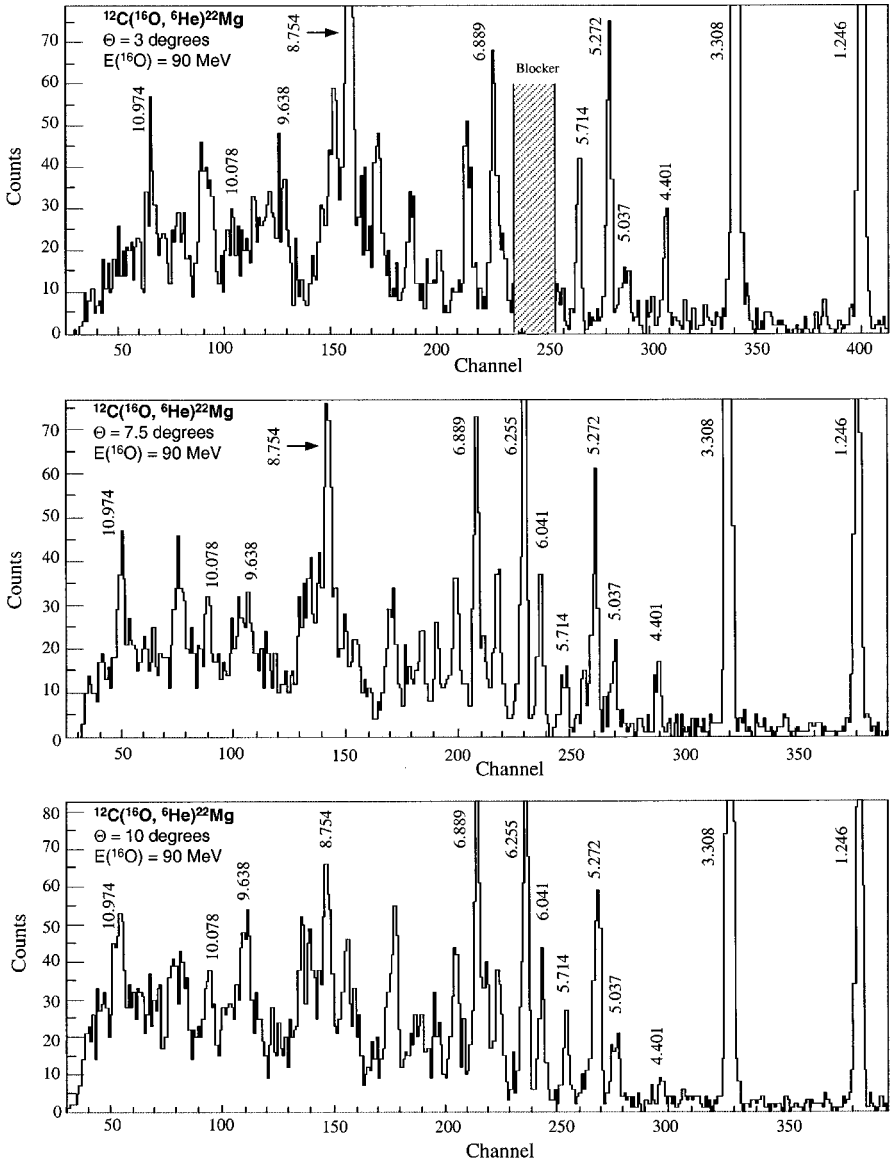

FIG. 4. Energy spectra obtained from the ^{12}C(^{16}O, ^{6}He)^{22}Mg reaction at 3°, 7.5°, and 10°. The states with asterisks were used in the energy calibration (see text for details). For the 3° spectrum, a 3.75-cm aluminum blocker was inserted in the focal plane to prevent elastically scattered beam particles from contaminating the spectrum.

with $E_x(^{22}\mathrm{Mg}) = 5-6$ MeV given in the 1990 $A=22$ compilation [4] have been retracted in the latest $A=22$ data supplement [18], and presently no mirror assignments in this region are listed. A comparison between levels in ^{22}Mg and ^{22}Ne, incorporating the present results, is shown in Fig. 6. The $E_x(^{22}\mathrm{Mg}) = 5.714$ MeV ($J^\pi = 2^+$) level has usually been considered to be the mirror of the $E_x(^{22}\mathrm{Ne}) = 6.115$ MeV ($J^\pi = 2^+$) level, since this state in ^{22}Ne is the only 2^+ state in this energy region. The $E_x = 5.965$ MeV level in ^{22}Mg, as listed in Ref. [4], in turn has traditionally been assigned as the mirror of the $E_x = 6.237$ MeV (0^+) state in ^{22}Ne, but with the recent results pointing to the existence of two levels at $E_x = 5.962$ and 6.046 MeV in ^{22}Mg, the situation is now more confused. In an earlier (p,t) measurement [17], a state at 6.06(±.04)MeV appears to have $J^\pi = 0^+$, and we therefore tentatively assign the $E_x = 6.237$ MeV ^{22}Ne level as the isospin mirror of the 6.046 MeV ^{22}Mg state. Note that the next highest $J^\pi = 0^+$ level in ^{22}Ne is located at $E_x = 6.90$ MeV and is therefore unlikely to be the mirror of the $E_x(^{22}\mathrm{Mg}) = 6.046$ MeV level.

Neither the present study nor the TRIUMF-CNS (p,t) measurement observed the $E_x(^{22}\mathrm{Mg}) = 5.837$ MeV state. If the existence of missing states in ^{22}Ne is precluded, then the only remaining state of ^{22}Ne in this energy region has $E_x(^{22}\mathrm{Ne}) = 5.910$ MeV and $J^\pi = 3^-$. This state in ^{22}Ne used to be assigned to the $E_x(^{22}\mathrm{Mg}) = 5.837$ MeV state [4], although presently, in light of the discussion above, this assignment is no longer warranted.

V. DISCUSSION

A. The ^{18}Ne$(\alpha,p)^{21}$Na reaction

The results from the present ^{12}C(^{16}O, ^{6}He)^{22}Mg reaction study extend the level scheme of natural parity states in the ^{22}Mg well into the energy region of relevance for resonances in the ^{18}Ne+α channel at the temperatures ($T \geqslant 0.5$ GK) found in x-ray bursts (Fig. 5). Our experimentally determined resonance energies have been used to improve the ^{18}Ne$(\alpha,p)^{21}$Na reaction rate that was first calculated by Görres and collaborators [5], using the narrow resonance formalism.

TABLE I. Excitation energies in ^{22}Mg with $E_x \geq 8.14$ MeV.

^{12}C(^{16}O, ^{6}He)^{22}Mg [a] E_x(MeV±keV)	^{20}Ne(^{3}He,n)^{22}Mg [b] E_x(MeV±keV)	^{18}Ne(α,p)^{22}Mg [c] E_x(MeV±keV)
8.203±23		
	8.290±40	
8.396±15		
8.547±18	8.550±90	
8.613±20		
8.754±15		
8.925±19		
9.066±18		
(9.172±23) [d]		
(9.248±20) [d]		
9.329±26		
(9.452±21) [d]		
9.533±24		
9.638±21		
9.712±21		
9.827±44		
9.924±28		
10.078±24		
10.190±29		
10.297±25		
10.429±26		
10.570±25		(10.580±50) [d]
10.660±28		
10.750±31		
10.844±38		(10.820±60) [d]
		10.910±50
10.980±31		10.990±50
		(11.050±50) [d]
11.135±40		11.130±50

[a]Present paper.
[b]From Alford *et al.* [14].
[c]From Bradfield-Smith *et al.* [3].
[d]Levels in parentheses are tentatively assigned.

1. Rate calculation

The treatment of stellar reactions using the narrow resonance formalism gives the following expression for the stellar reaction rate

$$N_A\langle\sigma\nu\rangle = 1.54\times10^{11}(\mu T)^{3/2}\sum_r (\omega\gamma)_{res} \times \exp(-11.605E_r/T_9)[\mathrm{cm^3 s^{-1}\ mol^{-1}}], \quad (1)$$

where μ is the reduced mass in u, $(\omega\gamma)_{res}$ is the resonance strength in units of MeV, E_{res} is the resonance energy, also in units of MeV, and T is the temperature in units of GK. The resonance strength is determined from the partial widths for the entrance and exit channels, Γ_{in} and Γ_{ex}, respectively, and the total resonance width, Γ_{tot}

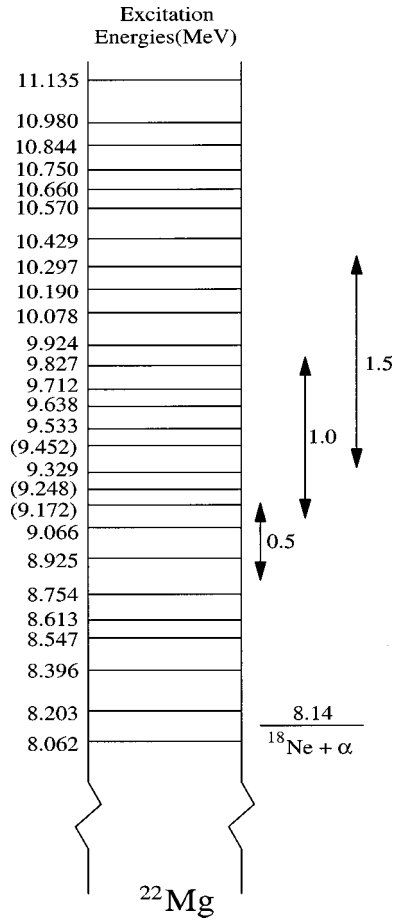

FIG. 5. Level scheme of ^{22}Mg showing the results from the present study. The Gamow energy windows for $T=0.5$, 1.0, and 1.5 GK are shown.

$$(\omega\gamma)_{res} = \frac{2J+1}{(2j_p+1)(2j_t+1)}\frac{\Gamma_{in}\Gamma_{ex}}{\Gamma_{tot}}, \quad (2)$$

where J, j_p, and j_t are the spins of the resonance state, the projectile, and the target, respectively. In calculating the ^{18}Ne(α,p)^{21}Na reaction rate using this formalism, knowledge of the proton partial widths is not required, since the resonance strength depends on the factor $\Gamma_\alpha\Gamma_p/\Gamma_{tot}$ and based on our knowledge of the states in ^{22}Ne, $\Gamma_\alpha \ll \Gamma_p \approx \Gamma_{tot}$, so that $\omega\gamma = \omega\Gamma_\alpha$. The partial α widths Γ_α are given by

$$\Gamma_\alpha = \frac{3\hbar^2}{\mu R^2} P_l C^2 S_\alpha, \quad (3)$$

where R is the nuclear interaction radius, P_l is the Coulomb penetrability factor, S_α is the α-spectroscopic factor, and C is the isospin Clebsch-Gordon coefficient. In the penetrability calculations, the nuclear interaction radius was calculated with the expression

$$R = 1.35(A_T^{1/3} + A_p^{1/3}), \quad (4)$$

TABLE II. Excitation energies in ^{22}Mg with $E_x \leq 8.14$ MeV.

^{12}C(^{16}O, ^{6}He)^{22}Mg [a] E_x(MeV±keV)	^{24}Mg(p,t)^{22}Mg [b] E_x(MeV±keV)	^{20}Ne(^{3}He,$n\gamma$)^{22}Mg [c] E_x(MeV±keV)	$A=22$ energy levels [d] E_x(MeV±keV)	J^π
1.2463 [e]		1.2470±0.4	1.2463±0.6	2^+
3.3082 [e]		3.3082±0.9	3.3082±0.8	$4^+(2^+)$
4.408[e]±12	4.3998±4.2	4.4019±1.5	4.4009±1.4	$2^+(1^+)$
		5.006±2	5.006±2	(0^+-4^+)
5.029[e]±12	5.0370 [e]	5.0370±1.4	5.0370±1.4	2^+
	5.0897±1.7			
5.272±9	5.2957±1.6	5.290±2	5.292±3	$(2^+,3)$
		5.317±5	5.317±5	(1–3)
	5.4543±1.6	5.464±5	5.464±5	(1–3)
5.711[e]±13	5.7139 [e]	5.7144±1.5	5.7139±1.2	2^+
		5.837±5	5.837±5	≤ 5
	5.9619±2.5		5.965±25	0^+
6.041±11	6.0458±3.0			
6.255±10	6.2464±5.1	6.298±50	6.267±15	4^+
	6.3226±6.0			
6.606±11	6.613±7		6.585±35	
6.767±20	6.787±14		6.783±19	3^-
6.889±10			6.980±80	3^-
7.169±11			7.213±18	0^+
7.402±13				
7.674±18				
7.784±18			7.840±90	
7.964±16			7.945±45	
8.062±16				

[a]Present paper.
[b]Levels from Bateman *et al.* [11].
[c]Levels from Rolfs *et al.* [15].
[d]$A=22$ energy levels compilation [4].
[e]Used for energy calibration.

where A_T and A_p are the atomic masses of the target and projectile, respectively.

In the Görres *et al.* calculation, given the complete lack of level information in the region of interest in ^{22}Mg, the energies for the ^{22}Mg resonances were determined simply by shifting the energies of known natural-parity states in the mirror ^{22}Ne by a fixed amount (about 200 keV). In the present calculation, the resonance energies used are those measured in our ^{12}C(^{16}O,^{6}He)^{22}Mg experiment, and the Coulomb penetrabilities have been recalculated to reflect these new energies. The same ^{22}Ne level parameters were used as in Görres *et al.* to infer the properties of the corresponding ^{22}Mg states, and therefore any differences in the reaction rates are due solely to changes in the resonance energies.

The resonance parameters used in our reaction rate calculation are listed in Table III. The energies of the ^{22}Mg states in the first column correspond to excitation energies found in the present study, and the levels in ^{22}Ne (which were arbitrarily chosen to correspond to known natural-parity states whose energies fall in the range of importance to the ^{18}Ne(α,p)^{21}Na rate for $T=0.2$–1.0 GK) are listed in the second column. (Although higher-lying states have been located in the present paper, there is no spectroscopic information available for these resonances from the present measurements or from the earlier measurements in ^{22}Ne. Therefore, their contributions to the ^{18}Ne(α,p) reaction rate cannot yet be determined, and our (α,p) rate calculation must be limited to $T \leq 1.0$ GK.) The ^{22}Ne spin and parity assignments are taken from the literature [4], or were determined from angular distributions of the ^{18}O(^{6}Li,d)^{22}Ne reaction [19]. The ^{22}Mg α-spectroscopic factors were calculated by Görres *et al.* [5] using the S_α (spectroscopic factors) from the ^{18}O(^{6}Li, d)^{22}Ne study. The spectroscopic factors listed in Table III include corrections to the ones listed by Görres *et al.* for the $E_x=9.725$ and 9.842 MeV levels in ^{22}Ne, since in their paper these two resonances have spectroscopic factors that are too small by a factor of 3 [20]. The Coulomb penetrabilities for the new resonance energies were recalculated and new values for the resonance strengths were determined.

The resulting ^{18}Ne(α,p)^{21}Na reaction rate, together with the results from previous rate calculations, are plotted in Fig. 7. The previous calculations include (a) the old level parameter calculation by Görres *et al.* [5], (b) a calculation of the rate using a statistical model approach [5], and (c) the reaction rate calculated from the results of the direct measurement of the ^{18}Ne(α,p)^{21}Na reaction by Bradfield-Smith and collaborators. This last rate calculation included only the lev-

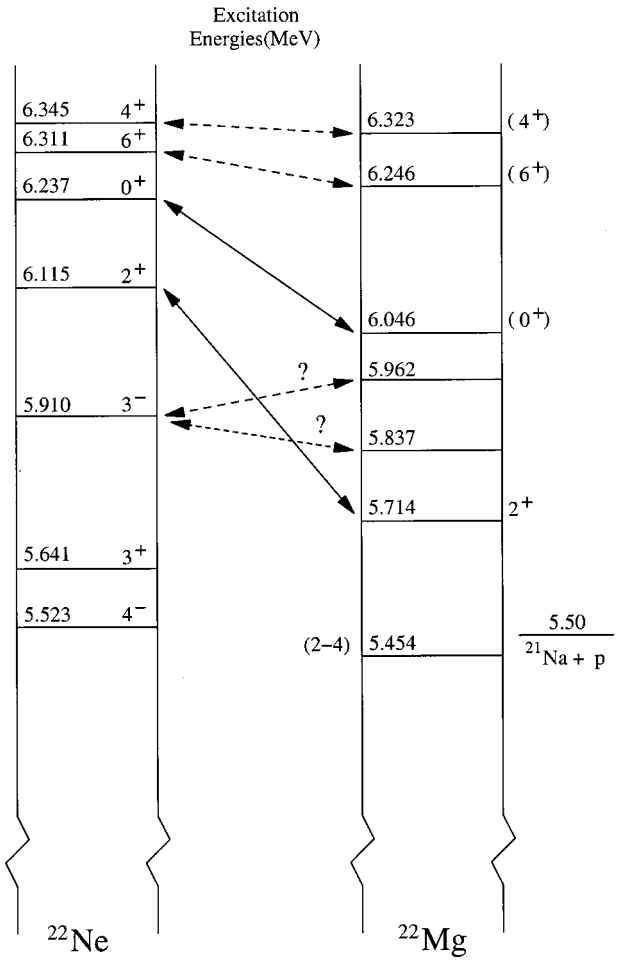

FIG. 6. Mirror assignments for levels relevant to ^{21}Na$(p,\gamma)^{22}$Mg. The states in ^{22}Mg include results from the present study and from Ref. [11]; the adopted energies are taken from Ref. [11]. The states in ^{22}Ne are taken from Ref. [4]. The assignments shown with solid double arrows are firm, while those with dashed ones are tentative.

els measured above $E_x \sim 10.5$ MeV. While these resonances were found to dominate the rate for temperatures above 2.5 GK (near the peak temperatures reached during an x ray burst), the exclusion of lower-energy resonances in their calculations results in a severe underprediction of the

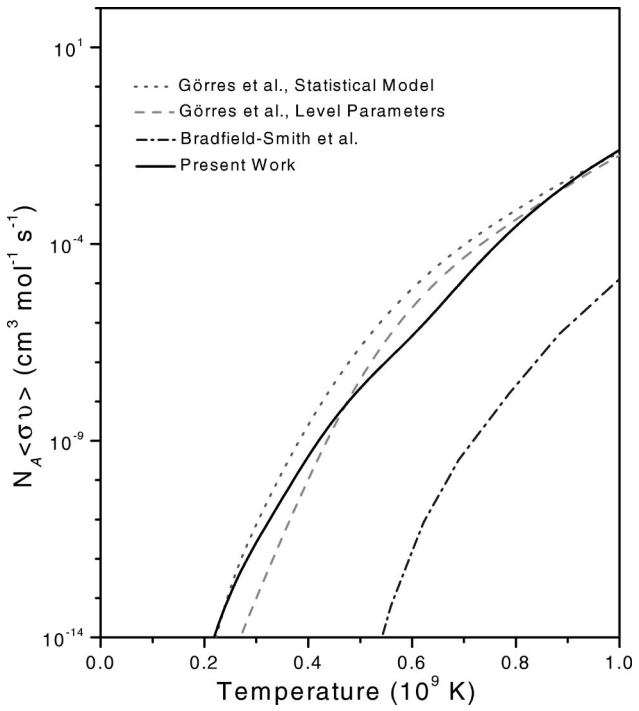

FIG. 7. The ^{18}Ne$(\alpha,p)^{21}$Na reaction rate as a function of temperature. The rate derived from the present study is plotted in comparison with those calculated in Refs. [3,5].

^{18}Ne$(\alpha,p)^{21}$Na reaction rate at lower temperatures. Furthermore, Fig. 7 illustrates the importance of precise resonance energies in reaction rate calculations, since, as an example, the reaction rate calculated in the present study is different from the corresponding level-parameter calculation of Görres *et al.* by factors of 10–100.

The comparison in Fig. 7 shows the anticipated contribution of resonances at energies below those measured by Bradfield-Smith *et al.* to the ^{18}Ne$(\alpha,p)^{21}$Na reaction rate in the temperature range $T=0.2$–1.0 GK, covering the temperature range corresponding to the possible breakout from the Hot-CNO cycle to the rp process. Our results point to the possibility that at temperatures below 0.5 GK, any ^{18}Ne present in the stellar environment will be processed via the ^{18}Ne$(\alpha,p)^{21}$Na reaction substantially more quickly than previously thought. In Fig. 8, a contour is plotted in density-

TABLE III. Resonance parameters for the ^{18}Ne$(\alpha,p)^{21}$Na reaction rate calculation.

$E_x(^{22}\mathrm{Mg})$(MeV) [a]	$E_x(^{22}\mathrm{Ne})$(MeV) [b]	J^π [c]	E_{res}(c.m.)(MeV)	S_α [c]	$\omega\gamma$(eV)
8.547	8.596	2^+	0.407	0.225	9.4×10^{-11}
8.613	8.741	3^-	0.473	0.012	5.3×10^{-11}
8.754	8.976	4^+	0.614	0.06	1.6×10^{-8}
8.925	9.097	3^-	0.785	0.045	2.2×10^{-5}
9.638	9.725	3^-	1.498	0.033	0.95
9.712	9.842	2^+	1.572	0.03	6.4
9.827	10.066	0^+	1.687	0.45	268.7

[a]From the present paper.
[b]From Ref. [19].
[c]From Ref. [5].

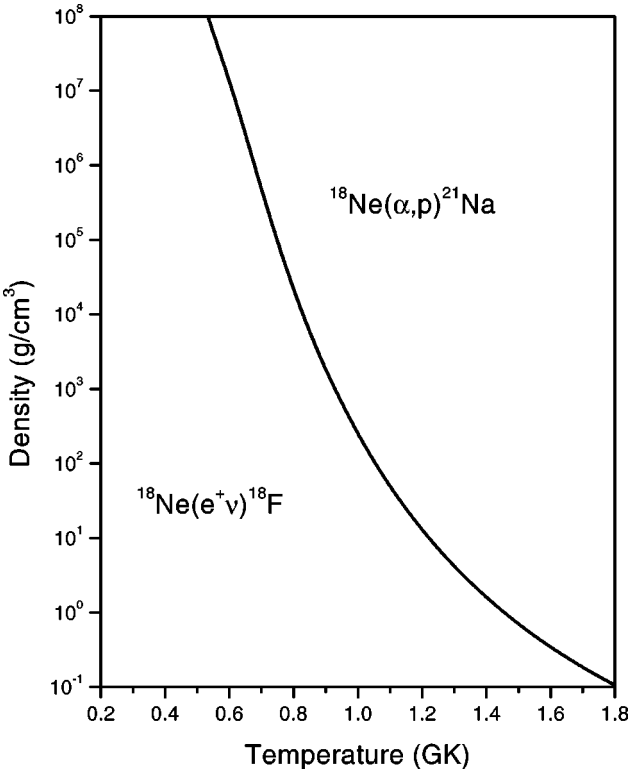

FIG. 8. Contour in density-temperature space at which the β-decay rate of ^{18}Ne is equal to the ^{18}Ne$(\alpha,p)^{21}$Na reaction rate. The curve shown is for a helium mass fraction of 0.27 (solar composition).

temperature space corresponding to the values of temperature and density for which the rates of ^{18}Ne destruction through β decay and through the ^{18}Ne$(\alpha,p)^{21}$Na reaction are equal, assuming a solar composition for the accreted material. To the right of the contour, mass flow to $A>19$ (to the rp process) occurs through the ^{18}Ne$(\alpha,p)^{21}$Na reaction. To the left, material is recycled back to ^{15}O in the Hot-CNO cycle. Since the typical densities on the surface of the accreting neutron star for an x-ray burst are in the range 10^5-10^7 g/cm^3, breakout from the Hot-CNO cycle through ^{18}Ne$(\alpha,p)^{21}$Na is seen to occur in the temperature range $T=0.6$–0.8 GK. It should also be noted that the amount of ^{18}Ne present in the stellar environment is determined by the reaction sequence ^{14}O$(\alpha,p)^{17}$F$(p,\gamma)^{18}$Ne. Both of these reactions have been subjects of intensive study in stable beam spectroscopy [13], and initial radioactive ion-beam studies [21,22] have also been performed to determine their respective stellar reaction rates.

2. Uncertainties in the reaction rate

The conclusions above are contingent on the following caveats:

(1) There may be missing natural-parity states in both ^{22}Mg and ^{22}Ne in the region of interest that may further increase the rate of the ^{18}Ne$(\alpha,p)^{21}$Na reaction. For example, there are five resonances in ^{22}Ne with excitation energies between 9–9.7 MeV that could not be included in our rate estimates because the spins and parities of these states are presently unknown. The present estimate, however, can be considered as a lower limit for the rate.

(2) The J^π assignments for some of the ^{22}Ne states used to determine the properties of mirror states in ^{22}Mg are tentative, since in some instances the fits to angular distributions from the ^{18}O$(^6$Li$,d)^{22}$Ne are ambiguous [19]. In those cases, the spin assignments were based on the relative quality of the fits. Since the resonance strength contains a statistical factor that is dependent on the spins of the resonances selected, this ambiguity could lead to uncertainties in the rate calculation.

(3) One must also be careful about assuming that the α spectroscopic factors for isospin mirror states are identical. This was assumed in our calculation due to the lack of experimental information on the α spectroscopic factors of the ^{22}Mg states. Other studies have shown that such model-dependent assumptions can lead to significant uncertainties [23].

(4) The mirror assignments assumed in the calculation may be incorrect.

These factors lead to uncertainties in the reaction rate that are difficult to quantify, since the available level parameter information is sparse. One should note that a statistical model generally gives reliable results when applied to situations where at least ten resonances contribute in the Gamow energy window [24]. In the case of the ^{18}Ne$(\alpha,p)^{21}$Na reaction, this requirement would correspond to temperatures above $T\sim1.5$ GK. For temperatures below 1.5 GK, contributions from individual resonances need to be considered. The present experiment represents an attempt to place the ^{18}Ne$(\alpha,p)^{21}$Na rate at these lower temperatures on firmer experimental ground by at least locating those resonances.

3. ^{18}Ne$(\alpha,p)^{21}$Na: Future work

In order to better determine the ^{18}Ne$(\alpha,p)^{21}$Na rate and to gain a clearer picture of its role in explosive nucleosynthesis, further work on the structure of ^{22}Mg is needed. The reaction rate at high temperatures ($T\geqslant2.5$ GK) has been determined [3] by the direct measurement at Louvain-la-Neuve. For $T<2.5$ GK, the present work represents a step forward by determining the locations of natural-parity states in the corresponding energy region. Future experiments that will measure the spectroscopic properties of important resonances directly with radioactive beams can now use this information to locate the important resonances quickly.

As an example, the Edinburgh-Louvain collaboration has already used the present results in a measurement of the ^{18}Ne$(\alpha,p)^{21}$Na that extended to lower energies ($E_x\sim9.5$ MeV) [25]; the analysis of those data is currently still in progress. At Argonne National Laboratory, efforts are already underway to measure the ^{18}Ne$(\alpha,p)^{21}$Na reaction rate at lower excitation energies in ^{22}Mg by using a ^{21}Na beam to measure the inverse reaction ^{21}Na$(p,\alpha)^{18}$Ne [26], and at TRIUMF-ISAC a proposal has been submitted to carry out low-energy measurements with a ^{18}Ne beam [27]. Progress in determining the widths of important states can also be made by using stable beam reactions to populate these states, and then measuring their decay branching ratios. Such a measurement is currently in progress at Yale University using the split-pole spectrometer coupled to a large solid-angle

silicon array similar to the Louvain-Edinburgh Detector Array (LEDA).

4. The ^{21}Na(p,γ)^{22}Mg reaction

In the region just above the ^{21}Na$+p$ threshold, the main result of this ^{12}C(^{16}O, ^{6}He)^{22}Mg reaction study of ^{22}Mg is our confirmation of the TRIUMF-CNS ^{24}Mg (p,t) result of a state at 6.041 MeV$\pm$11 keV (500 keV above the ^{21}Na $+p$ threshold). Our results are also in agreement with the TRIUMF-CNS results in not observing the previously reported state at $E_x(^{22}\mathrm{Mg})=5.837$ MeV, also of possible importance to hydrogen burning in novae. Altogether, these results point to a confusing situation regarding the structure of ^{22}Mg and the assignment of mirror states in ^{22}Ne in this particular energy region.

Given the difficulties encountered in attempts to estimate theoretically the ^{21}Na$+p$ resonance energies (despite progress using shell-model calculations and isobaric multiplet mass equations) to the level of precision required for astrophysics calculations, in order to fully understand the role played by the ^{21}Na$(p,\gamma)^{22}$Mg reaction in novae, further measurements must be carried out to determine the spectroscopic properties and resonance strengths of the important resonances, and hence the reaction rate. The branching ratio measurements mentioned above, using stable beam reactions (currently in progress at Yale University) may allow one to determine the partial widths of the important states. With the impending availability of ^{21}Na beams at radioactive ion beam (RIB) facilities, one particularly useful probe for measuring resonance locations and properties is the study of ^{21}Na$+p$ elastic scattering in inverse kinematics. This method has the advantage of requiring only relatively modest beam intensities ($\sim 10^3$ to 10^5/s), and has already been successfully applied at Oak Ridge National Laboratory to measure spectroscopic properties in the ^{17}F $+p$ and ^{18}F$+p$ systems [21,28]. Once the locations of key resonances are established, a direct measurement of the ^{21}Na$(p,\gamma)^{22}$Mg will determine the corresponding resonance strengths directly. Such a measurement requires the use of higher intensity beams and of recoil mass separators with excellent beam rejection. Both ^{21}Na(p,p) and ^{21}Na(p,γ) measurements [29,30] are currently in the planning stages at the TRIUMF radioactive beam facility in Vancouver, Canada, using the ^{21}Na beam that is scheduled to come online early in 2001.

VI. CONCLUSIONS

Using the heavy-ion reaction ^{12}C(^{16}O, ^{6}He)^{22}Mg, we have measured the location of key resonances for the ^{18}Ne$(\alpha,p)^{21}$Na and ^{21}Na$(p,\gamma)^{22}$Mg reactions, of importance to explosive hydrogen burning in x-ray bursts and novae, respectively. In particular, we have found 18 new levels above the ^{18}Ne$+\alpha$ threshold, including those resonances that will dominate the rate at temperatures characteristic of breakout from the Hot-CNO cycles to the rp process in x-ray bursts. Our resulting reaction rate points to an enhanced mass flow through the ^{18}Ne$(\alpha,p)^{21}$Na reaction, by up to two orders of magnitude over previous estimates. In addition, with regard to the ^{21}Na$(p,\gamma)^{22}$Mg reaction, we have have confirmed the presence of a level at $E_x=6.041(11)$ MeV that lies within the region of astrophysical interest for explosive hydrogen burning in novae.

Further progress in our understanding of the nuclear mechanisms that drive stellar explosions will certainly follow from the development of radioactive ion-beam facilities around the world, as well as from stable-beam branching-ratio measurements of the decay properties of these resonances. In the interim, the present study is an example of the role of stable-beam reactions in measuring important spectroscopic information that aids the planning of present and future radioactive ion-beam experiments, and complements their results.

ACKNOWLEDGMENTS

The authors wish to thank W. Bradfield-Smith, C. Iliadis, and J. Görres for helpful discussions, as well as the technical staff at Yale for their assistance. This work was supported by U.S. Department of Energy Grant No. DE-FG02-91ER-40609.

[1] M. Wiescher, H. Schatz, and A. E. Champagne, Philos. Trans. R. Soc. London, Ser. A **356**, 2105 (1998).
[2] M. Wiescher, J. Görres, and H. Schatz, J. Phys. G **25**, 133 (1999).
[3] W. Bradfield-Smith, T. Davinson, A. DiPietro, A. M. Laird, A. N. Ostrowski, A. C. Shotter, P. J. Woods, S. Cherubini, W. Galster, J. S. Graulich, P. Leleux, L. Michel, A. Ninane, J. Vervier, J. Görres, M. Wiescher, J. Rahighi, and J. Hinnefeld, Phys. Rev. C **59**, 3402 (1999).
[4] P. M. Endt, Nucl. Phys. **A521**, 1 (1990).
[5] J. Görres, M. Wiescher, and F.-K. Thielemann, Phys. Rev. C **51**, 392 (1995).
[6] M. Politano, S. Starrfield, J. W. Truran, A. Weiss, and W. M. Sparks, Astrophys. J. **448**, 807 (1995).
[7] E. Zinner, in *Nuclei in the Cosmos III*, edited by M. Busso, R. Gallino, and C. M. Raitieri, AIP Conf. Proc. No. 327 (AIP, New York, 1995), p. 567.
[8] M. Wiescher, J. Görres, F.-K. Thielemann, and H. Ritter, Astron. Astrophys. **160**, 56 (1986).
[9] M. Wiescher and K. Langanke, Z. Phys. A **325**, 309 (1986).
[10] N. A. Smirnova and A. Coc, Phys. Rev. C **62**, 045803 (2000).
[11] N. P. T. Bateman, K. Abe, G. Ball, L. Buchmann, J. Chow, J. M. D'Auria, Y. Fuchi, C. Iliadis, H. Ishiyama, K. P. Jackson, S. Karataglidis, S. Kato, S. Kubono, K. Kumagai, M. Kurokawa, X. Liu, S. Michimasa, P. Strasser, and M. H. Tanaka, Phys. Rev. C **63**, 035803 (2001).
[12] J. A. Caggiano, J. P. Greene, K. E. Rehm, W. Bradfield-Smith, R. Lewis, D. W. Visser, and P. D. Parker (private communication).
[13] K. I. Hahn, A. Garcia, E. G. Adelberger, P. V. Magnus, A. D.

Bacher, N. Bateman, G. P. A. Berg, J. C. Blackmon, A. E. Champagne, B. Davis, A. J. Howard, J. Liu, B. Lund, Z. Q. Mao, D. M. Markhoff, P. D. Parker, M. S. Smith, E. J. Stephenson, K. B. Swartz, S. Utku, R. B. Vogelaar, and K. Yildiz, Phys. Rev. C **54**, 1999 (1996).

[14] W. P. Alford, P. Craig, D. A. Lind, R. S. Raymond, J. Ullman, C. D. Zafiratos, and B. H. Wildenthal, Nucl. Phys. **A457**, 317 (1986).

[15] C. Rolfs, R. Kraemer, F. Riess, and E. Kuhlmann, Nucl. Phys. **A191**, 209 (1972).

[16] A. B. McDonald and E. G. Adelberger, Nucl. Phys. **A144**, 593 (1970).

[17] R. A. Paddock, Phys. Rev. C **5**, 485 (1972).

[18] P. M. Endt, Nucl. Phys. **A633**, 1 (1998).

[19] U. Giesen, C. P. Browne, J. Görres, J. G. Ross, M. Wiescher, R. E. Azuma, J. D. King, J. B. Vise, and M. Buckby, Nucl. Phys. **A567**, 146 (1994).

[20] J. Görres (private communication).

[21] D. W. Bardayan, J. C. Blackmon, C. R. Brune, A. E. Champagne, A. A. Chen, J. M. Cox, T. Davinson, V. Y. Hansper, M. A. Hofstee, B. A. Johnson, R. L. Kozub, Z. Ma, P. D. Parker, D. E. Pierce, M. T. Rabban, A. C. Shotter, M. S. Smith, K. B. Swartz, D. W. Visser, and P. J. Woods, Phys. Rev. Lett. **83**, 45 (1999).

[22] B. Harss, J. P. Greene, D. Henderson, R. V. F. Janssens, C. L. Jiang, J. Nolen, R. C. Pardo, K. E. Rehm, J. P. Schiffer, A. A. Sonzogni, J. Uusitalo, I. Wiedenhver, M. Paul, T. F. Wang, F. Borasi, R. E. Segel, J. Blackmon, M. Smith, A. Chen, and P. Parker, Phys. Rev. Lett. **82**, 3964 (1999).

[23] F. de Oliveira, A. Coc, P. Aguer, G. Bogaert, J. Keiner, A. Lefebvre, V. Tatischeff, J.-P. Thibaud, S. Fortier, J. M. Maison, L. Rosier, G. Rotbrd, J. Vernotte, S. Wilmes, P. Mohr, V. Kölle, and G. Staudt, Phys. Rev. C **55**, 3149 (1997).

[24] T. Rauscher, F.-K. Thielemann, and K.-L. Kratz, Phys. Rev. C **56**, 1613 (1997).

[25] A. C. Shotter, private communication.

[26] K. E. Rehm, B. Harss, N. Bateman, F. Borasi, R. Janssens, C. L. Jiang, J. Nolen, R. Pardo, P. Parker, M. Paul, P. Reiter, J. Schiffer, R. Segel, A. Sonzogni, J. Uusitalo, and I. Wiedenhöver, approved ATLAS proposal, Argonne National Laboratory, 1998.

[27] A. C. Shotter, J. M. D'Auria, N. P. T. Bateman, R. N. Boyd, L. Buchmann, U. Giesen, U. Greife, R. Helmer, D. Hunter, A. Hussein, D. Hutcheon, K. P. Jackson, J. D. King, R. Korteling, S. Kubono, T. Motobayashi, A. Olin, P. D. Parger, C. Rolfs, J. Rogers, G. Roy, A. Shotter, F. Strieder, H.-P. Trautvetter, and M. Wiescher, Proposal E870 to the TRIUMF EEC, 1999.

[28] D. W. Bardayan, J. C. Blackmon, W. Bradfield-Smith, C. R. Brune, A. E. Champagne, T. Davinson, B. A. Johnson, R. L. Kozub, C. S. Lee, P. D. Parker, A. C. Shotter, M. S. Smith, D. W. Visser, and P. J. Woods, Phys. Rev. C **62**, 042802(R) (2000).

[29] L. Buchmann *et al.*, Proposal E879 to the TRIUMF EEC, 1999.

[30] J. M. D'Auria, N. P. T. Bateman, R. N. Boyd, L. Buchmann, U. Giesen, U. Greife, R. Helmer, D. Hunter, A. Hussein, D. Hutcheon, K. P. Jackson, J. D. King, R. Korteling, S. Kubono, T. Motobayashi, A. Olin, P. D. Parker, C. Rolfs, J. Rogers, G. Roy, A. Shotter, F. Strieder, H.-P. Trautvetter, and M. Wiescher, Proposal E824 to the TRIUMF EEC, 1997.